Towards the Computer-Aided Molecular Design of Organic Rankine Cycle Systems with Advanced Fluid Theories

Oyeniyi A. Oyewunmi, Andrew J. Haslam and Christos N. Markides *

Clean Energy Processes (CEP) Laboratory, Department of Chemical Engineering, Imperial College London, London SW7 2AZ, United Kingdom

* Corresponding author. Email: c.markides@imperial.ac.uk; Tel. +44 (0)20 759 41601

Abstract

Organic Rankine cycle (ORC) power-generation systems are increasingly being deployed for heat recovery and conversion from geothermal reservoirs and in several industrial settings. Using a case study of an exhaust flue-gas stream, an ORC power output in excess of 20 MW is predicted at thermal efficiencies ranging between 5% and 15%. The considerable influence on cycle performance of the choice of the working fluid is illustrated with alkane and perfluoroalkane systems modelled using the SAFT-VR Mie equation of state (EoS); in general, the more-volatile pure components (*n*-butane or *n*-perfluorobutane) are preferred although some mixtures perform better at restricted cycle conditions.

The development of computer-aided molecular design (CAMD) platforms for ORC systems requires both cycle and working-fluid models to be incorporated into a single framework, for the purposes of whole-system design and optimization. Using pure alkanes and their mixtures as a case study, we test the suitability of the recent group-contribution SAFT-γ Mie EoS method for describing the thermodynamic properties of working fluids relevant to the analysis of ORC systems. The theory is shown to predict accurately the relevant properties of these fluids, thereby suggesting that this SAFT-based CAMD approach is a promising approach towards working-fluid design of ORC power systems.

Keywords heat recovery, SAFT-γ Mie, group contribution, ORC, SAFT-VR Mie, CAMD

1 Introduction

Recent trends in global energy usage have shown rapid increases, especially in developing countries, accompanied by steadily rising energy prices due to a combination of growing energy demands and the depletion of easily accessible fossil-fuel reserves. These challenges, along with environmental concerns associated with the consumption of fossil fuels, will continue to act as important drivers behind the interest in low-grade (up to 300 °C) heat and its subsequent conversion to power. In particular, the utilization of low-grade waste heat has been identified as one of the major pathways towards a high-efficiency and sustainable energy future [1]. Developing waste-heat technologies also promotes the harnessing of low-grade heat from renewable sources (e.g., solar, geothermal).

Presently, vast amounts of low-grade heat (in the form of exhaust gases, cooling streams, *etc*.) are disposed of to the biosphere from a diverse range of sources in the domestic, commercial, industrial and transport sectors. Recent estimates show that over 60% of the energy generated from various renewable and non-renewable sources is rejected into the atmosphere; the largest contributors are electrical power plants, transportation and oil refining. Specifically, 59.0 Quads (~ 62×10^{18} J) of energy were 'rejected' to the atmosphere in the U.S. in the year 2013 [2]. This exceeds the actual energy consumed (38.4 Quads) by over 50%. Similar figures were reported for Europe and Asia [3].

Heat engines utilizing low-temperature heat-sources are inherently inefficient. The Chambadal-Novikov efficiency [4, 5] for source temperatures in the range 100-300 °C varies between 10% and 27%, which is notably lower than (conventional) power plants. Nevertheless, low-grade heat engines can play a crucial role in increasing industrial efficiency and the use of sustainable energy resources such as solar and geothermal heat, as well as in reducing the rate at which non-renewable resources are being depleted and consumed, and also at which associated harmful gaseous emissions are being released to the atmosphere. Re-using waste heat has the potential to provide an additional 8 EJ of energy towards the annual consumption in Europe, corresponding to over 15% of annual energy usage.

A number of waste-heat power-generation technologies are based on the Rankine cycle and its variants, including the organic Rankine cycle (ORC), the Kalina cycle and the supercritical CO_2 cycle. These engines differ from (steam) Rankine-cycle engines chiefly in their choice of working fluid (WF) – those based on the Kalina cycle utilize a mixture of water and ammonia, while ORC engines utilize organic fluids and their mixtures. The ORC WF is usually a 'dry' or 'isentropic' organic fluid – *i.e.*, a fluid for which the dry saturation line or dew-point curve in temperature-entropy (*T*-*s*) space has a positive slope. Such fluids do not need to be superheated to avoid condensation in the turbine, as is required with water (a 'wet' fluid) in a conventional steam Rankine-cycle system.

The choice of organic WF has a considerable impact on the design, performance and economics of ORC systems, thus, a considerable body of work has and continues to be dedicated to the study of suitable fluids for different applications [6-9]. The general approach has been to investigate known fluids with available thermophysical properties in different ORC system configurations. The suggested WFs include hydrocarbons, refrigerants and siloxanes [8-11]. This approach, however, limits the flexibility in the design of WFs for ORCs, especially when one considers the possible use of fluid mixtures. The development of advanced fluid theories rooted in interactions on the molecular scale provides an opportunity for the intelligent design of WFs for any ORC configuration [12-15].

In this paper, we deploy the molecular-based SAFT-VR Mie equation of state (EoS) [16], for the accurate prediction of the thermodynamic properties of organic WFs. SAFT-VR Mie is shown (by comparison with experimental data) to predict accurately both single-phase and saturation properties of these fluids and their mixtures, including their second-derivative properties (e.g., specific heat capacities), which are more challenging and less reliably calculated by cubic EoS. This enables an accurate description of important WF properties (entropies, enthalpies, heat capacities) and thus of the performance of associated ORC engines. We proceed also to introducing the SAFT-γ Mie group-contribution EoS [17, 18] as a method for the accurate prediction of WF thermodynamic properties. This EoS can allow the flexibility of designing WFs from their constituent functional groups which, in turn, will enhance the capabilities of computer-aided molecular design (CAMD) tools for the development of innovative architectures and whole-system optimization of ORC engines, including the design of novel cycles and novel WFs for targeted applications.

2 SAFT-VR Mie Equation of State

The prediction of the thermo-physical properties of fluid systems is particularly important in many engineering applications especially as single-component fluids are used in many industrial systems. Experimental thermodynamic data for a wide range of such pure-fluid systems can be reliably obtained from sources such as the NIST/TRC Web Thermo Tables [23]. On the other hand, experimental data for fluid mixtures are not plentiful, especially in relation to calorific quantities such as those required when designing WFs for heat engines such as the ORC. Traditionally, cubic EoS [19, 20] have been widely employed in modelling properties of fluid systems. Although they have been reliably used over the years for the description of phase-equilibrium properties in *P*-*T*-*x* space, they are less accurate when predicting calorific properties for both single-component and multi-component fluid systems. Moreover, they are less dependable in predicting second-derivative properties such as heat capacity, isothermal compressibility and the coefficient of thermal expansion.

The need for an all-encompassing description of the thermodynamics of a fluid has driven the development of molecular-based EoS, incorporating more-realistic representations of the interactions between fluid molecules than is implicit in the semi-empirical cubic EoS. The statistical associating fluid theory (SAFT) EoS [21] has a firm basis in statistical mechanics, allowing it to provide a predictive capability lacked by cubic EoS. In this work we employ the state-of-the-art SAFT-VR Mie EoS for the prediction of thermodynamic information. This EoS provides a very accurate description of the densities and phase-change enthalpies of typical ORC WFs, including alkanes and perfluoroalkanes [16] as considered in this work, thus giving confidence that it is suitable for calculating the calorific quantities required for an ORC simulation.

In SAFT-VR Mie, the fluid molecules are modelled as chains of m spherical segments that interact via a Mie pair potential, ϕ, defined as:

$$\phi(r) = \frac{\lambda_r}{\lambda_r - \lambda_a}\left(\frac{\lambda_r}{\lambda_a}\right)^{\frac{\lambda_a}{\lambda_r-\lambda_a}} \varepsilon \left[\left(\frac{\sigma}{r}\right)^{\lambda_r} - \left(\frac{\sigma}{r}\right)^{\lambda_a}\right]. \qquad [1]$$

Here, r represents the separation of the two interacting segments, σ is a parameter representing the size of the segment, ε is the depth of the potential well, and the remaining molecular-model parameters, λ_r and λ_a are respectively the repulsive and attractive exponents characterizing the range of the potential. The Mie potential reduces to the familiar Lennard-Jones potential for the case $\lambda_r = 12$ and $\lambda_a = 6$. These intermolecular parameters define the underlying model of non-associating pure fluids. In particular, SAFT-VR Mie facilitates the adjustment of the repulsive exponent λ_r to suit the relative hardness or softness of a molecule thereby enabling an accurate description of second derivative properties (such as heat capacity and by extension, the specific entropy) which are important in exploring heat engines. Similar to other versions of SAFT, SAFT-VR Mie enables one to calculate the Helmholtz free energy of a fluid as a sum of ideal and residual contributions. The residual contribution is a sum of individual contributions from the monomer segments, the grouping of segments into chains and an association term in the case of associating molecules. Mixtures are treated using van der Waals one-fluid mixing rules, with standard combining rules. Further details concerning SAFT-VR Mie, including the model parameters for the fluids investigated here, can be found in Ref. [16]. Thermodynamic quantities of interest such as enthalpies, entropies and chemical potentials are obtained from the Helmholtz free energy using standard thermodynamic relations.

The effectiveness of the approach is illustrated in Figs. 1 and 2, which demonstrate the accuracy of the SAFT-VR Mie EoS in predicting important properties required for ORC analysis for the case of *n*-butane, *n*-decane and their mixtures. SAFT-VR Mie predictions (curves) are compared with available experimental data taken from the NIST database [23] (symbols).

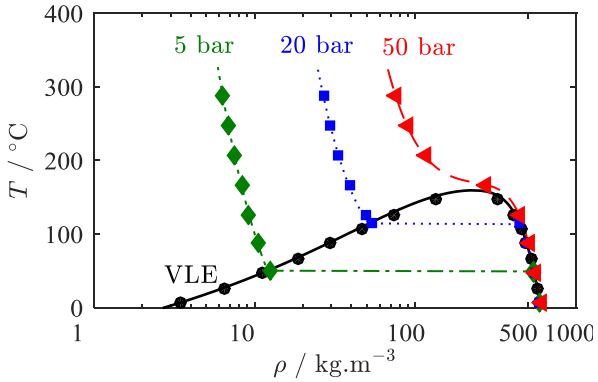


Fig. 1a: *VLE and isobaric T-ρ plots for n-butane*

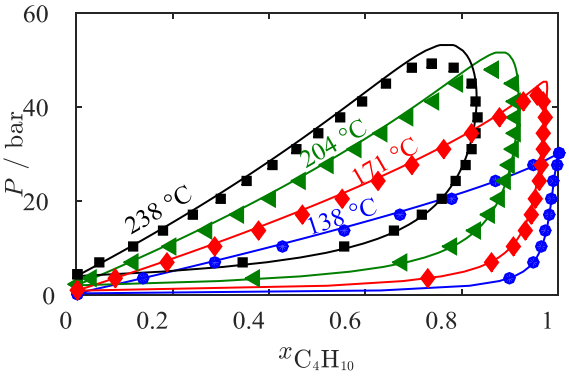


Fig. 1b: *Isothermal P-x phase boundaries for n-butane + n-decane system*

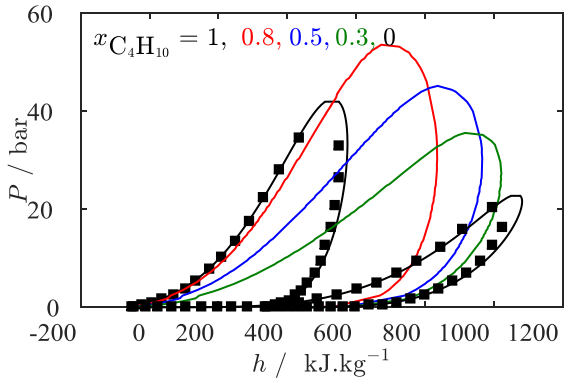


Fig. 2a: *P-h phase boundaries for n-butane + n-decane system*

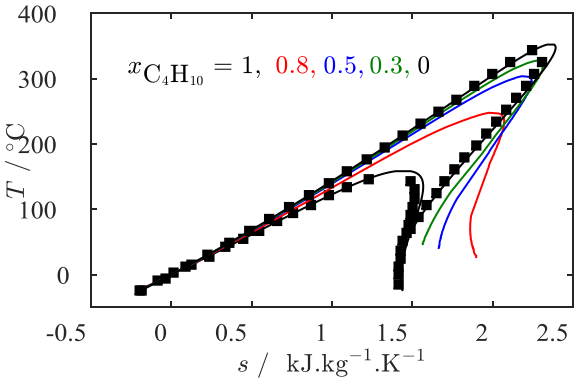


Fig. 2b: *T-s phase boundaries for n-butane + n-decane system*

In more detail, Fig. 1 shows the vapour-liquid temperature-density (T-ρ) coexistence envelope and density isobars (P = 5, 20 and 50 bar) for *n*-butane calculated with SAFT-VR Mie. Isothermal pressure-composition (P-x) envelopes of *n*-butane + *n*-decane are presented in Fig. 1b together with data from the experimental measurements of Reamer and Sage [24]. The verification is concluded by predicting the phase equilibria of the alkane mixtures in temperature-entropy (T-s) and pressure-enthalpy (P-h) spaces. In Fig. 2a, predicted phase envelopes for both *n*-butane and *n*-decane are presented in P-h space, together with those of intermediate mixtures comprising 30, 50, and 80 mol% *n*-butane to illustrate the crossover in the phase behaviour between the two pure components. In Fig. 2b, these phase envelopes are provided in T-s space.

From Fig. 1, it can be observed that the description of the fluid density in all regions of interest – the condensed liquid and superheated-vapour phases – as well as the supercritical region, is excellent. Also, the phase equilibria of the fluid mixture are well described over a wide temperature range. The slight disagreement in the critical region at high temperatures is expected as it is well known that analytical EoS cannot simultaneously capture both the critical and subcritical regions [25]; nevertheless the description from SAFT-VR Mie remains very good. Save for correlative equations with very large numbers of parameters, this degree of agreement has hitherto not been possible using analytical EoS. The agreement between the calculated and experimental pure-component phase envelopes in Fig. 2 is especially promising since these experimental data were not considered during the refinement of the molecular model parameters. The quality of the agreement for *n*-butane and the *n*-butane + *n*-decane binary mixture as illustrated in Figs. 1 and 2 emphasizes the predictive power of the SAFT-VR Mie EoS modelling, providing confidence in the reliability of the thermodynamic-property predictions for working-fluid mixtures in ORC calculations.

3 Waste-Heat Recovery ORC Simulation Results

3.1 ORC thermodynamic model

As previously highlighted, the ORC, similarly to the steam cycle, consists of four processes carried out by an organic WF. A typical ORC setup with the associated T-s diagram is shown in Fig. 3, with the states of the WF at labelled points through the cycle are indicated on the T-s diagram. The model equations for each of the processes are summarized below the figure.

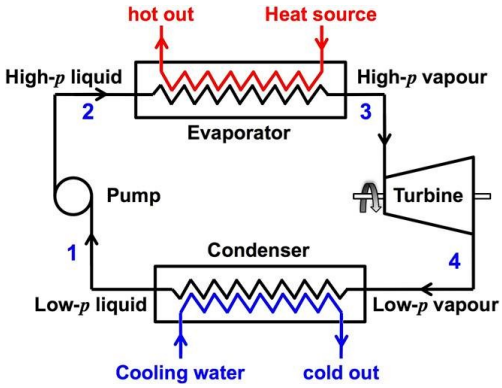


Fig. 3a: *Schematic diagram of ORC engine*

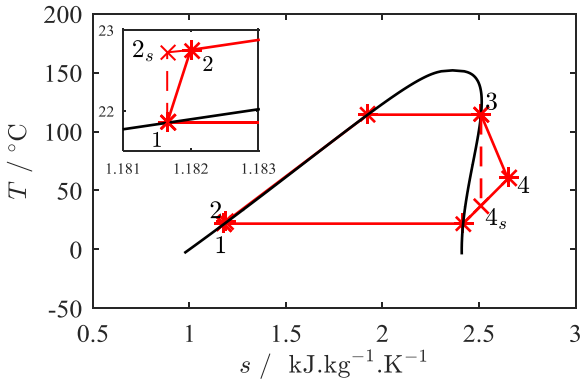


Fig. 3b: *ORC T-s diagram for pure (single-component) WF*

The power required to pump the WF from State 1 to State 2 is:

$$\dot{W}_{\text{pump}} = \dot{m}_{\text{wf}}(h_2 - h_1) = \dot{m}_{\text{wf}}(h_{2s} - h_1)/\eta_{\text{is,pump}} \,, \qquad [2]$$

where $\dot{m}_{\text{wf}}$ represents the mass flowrate of the WF and $\eta_{\text{is,pump}}$ is the isentropic efficiency of the pump, which is taken as 75% in the present study.

The heat extracted from the heat source is transferred to the WF assuming no heat losses and with a minimum pinch temperature difference of 10 °C in the evaporator. The WF exits the evaporator as a saturated vapour as depicted in Fig. 3b; it is not superheated as superheating has been shown to be

detrimental to ORC performance [13]. The heat extraction process is assumed to be isobaric (at P_{23}). Thus the rate of heat input from the heat source is given by:

$$\dot{Q}_{\text{in}} = \dot{m}_{\text{wf}}(h_3 - h_2) = \dot{m}_{\text{hs}} c_{\text{p,hs}}\left(T_{\text{hs,in}} - T_{\text{hs,out}}\right) . \quad [3]$$

Following heat addition, the WF expands through an expander to generate power. The isentropic efficiency of the expander, $\eta_{\text{is,exp}}$, is taken as 75% and the generated power is calculated as:

$$\dot{W}_{\text{exp}} = \dot{m}_{\text{wf}}(h_3 - h_4) = \eta_{\text{is,exp}} \dot{m}_{\text{wf}}(h_3 - h_{4\text{s}}) . \quad [4]$$

In the condenser, heat is rejected as the WF is first de-superheated and then condensed at constant pressure (at P_{41}) to a saturated liquid. The rate of heat transferred to a cooling stream is given as:

$$\dot{Q}_{\text{out}} = \dot{m}_{\text{wf}}(h_4 - h_1) = \dot{m}_{\text{cs}} c_{p,\text{cs}}\left(T_{\text{cs,out}} - T_{\text{cs,in}}\right) . \quad [5]$$

The conditions inside the condenser are set such that the pressure is not lower than atmospheric pressure, and the temperature is not lower than 30 °C. Thus,

$$P_{41} = \max\ \{1\ \text{bar}, P_{\text{bub,30 °C}}\}, \quad [6]$$

where $P_{\text{bub,30 °C}}$ is the bubble point pressure of the WF at 30 °C.

While the power output, $\dot{W}_{\text{exp}}$, serves as the primary performance index of interest in this study, the cycle thermal efficiency is also an equally important performance index. The thermal efficiency, η_{th}, of the investigated cycles is calculated as:

$$\eta_{\text{th}} = (\dot{W}_{\text{exp}} - \dot{W}_{\text{pump}}) / \dot{Q}_{\text{in}} . \quad [7]$$

In this present study, flue gas from a refinery gas-fired boiler – with a flowrate of 560 kg/s and temperature of 330 °C – is used as an example waste-heat stream composed largely of nitrogen and oxygen with traces of steam and carbon dioxide, with an average specific-heat capacity, c_p, of 1.07 kJ/kg.K. The cooling stream is water at 20 °C; its flowrate is suitably adjusted to ensure the condenser pinch conditions (set at a minimum of 10 °C) are satisfied.

3.2 Working fluid comparison

First, using the SAFT-VR Mie EoS, the WF thermodynamic properties are calculated as functions of P, T and x. These properties are then stored in look-up tables and accessed by the ORC model via interpolation. Using two sets of working-fluid mixtures – *n*-butane + *n*-decane and *n*-perfluorobutane + *n*-perfluorodecane – the ORC model is simulated in order to investigate the role of changes to the WF composition on system performance, as described below.

3.2.1 Thermal efficiency, specific power and expansion ratio

Presented in Fig. 4 are the specific work output ($w_{\text{c}} = \dot{W}_{\text{exp}}/\dot{m}_{\text{wf}}$), the thermal efficiency η_{th} and the expansion ratio ($V_{43} = V_4/V_3$) as functions of the mole fraction of the more volatile component – *n*-butane (or *n*-perfluorobutane) – in the working-fluid mixture, at different evaporating pressures (P_{23}). These properties are independent of $\dot{m}_{\text{wf}}$ and thus enable a direct comparison between ORC configurations. The specific work, w_{c}, gives an indication of the energy density of each configuration and how this varies with the WF mixture used, while V_{43} provides an indication of the size (and/or number of stages) of the expander required. A high V_{43} necessitates the use of a large expander or one comprising many stages which, in turn, leads to higher costs. By and large, both sets of working-fluid mixture exhibit similar trends in the performance indices.

For the two sets of WF, the pure components (x = 0 or x = 1) generally give rise to cycles of higher thermal efficiency than the WF mixtures, as evidenced in Fig. 4a for the alkanes. At evaporation pressures less than 10 bar, cycles with pure *n*-decane or *n*-perfluorodecane WFs are the most efficient whereas at higher evaporation pressures, cycles with pure *n*-butane or *n*-perfluorobutane exhibit the highest thermal efficiency. Cycles with working-fluid mixtures exhibit lower efficiencies varying between these extremes. One might have expected the mixtures to lead to cycles with higher thermal

efficiencies, especially as they have higher average heat addition temperatures (compared to single-component fluids) due to their non-isothermal heat evaporation. However, this also makes them to exhibit a higher average heat-rejection temperature, which is detrimental to the thermal efficiency.

For cost minimization, a cycle with a lower expansion ratio is preferred to one with a higher ratio. The expansion ratios for the WFs are illustrated in Fig. 4b for perfluoroalkanes. It is clear that the WF mixtures rich in the more-volatile component (*i.e.*, *n*-butane or *n*-perfluorobutane) lead to cycles with the lowest expansion ratios. At evaporating pressures lower than 6 bar, the cycles with *n*-butane or *n*-perfluorobutane WFs have the lowest expansion ratios; cycles with *n*-decane or *n*-perfluorodecane WFs have the highest expansion ratios and thus may lead to costlier systems even though they are more efficient. Cycles with a working-fluid mixture with 90 mol% of *n*-butane or *n*-perfluorobutane generally have the lowest expansion ratios and may be the most cost effective.

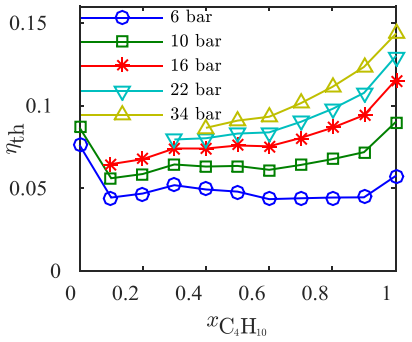


Fig. 4a: *Thermal efficiencies of ORCs with alkane WFs*

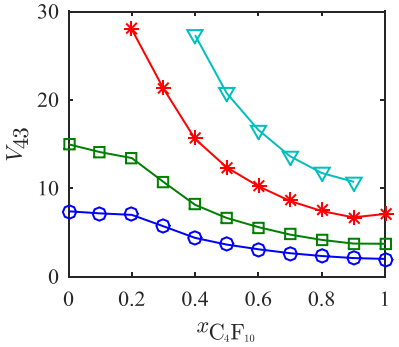


Fig. 4b: *Expansion ratios of ORCs with perfluoroalkane WFs*

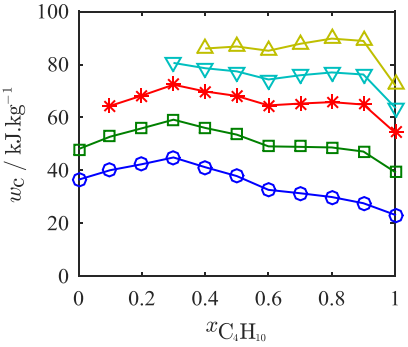


Fig. 4c: *Specific power output of ORCs with alkane WFs*

In Fig. 4c we illustrate the variation in w_c with the WF concentration. While the single-component WFs show a better performance in terms of η_{th}, the mixtures perform considerably better than their pure counterparts in terms of this performance index. For the perfluoroalkanes, a cycle of 20 mol% *n*-perfluorobutane consistently delivers the highest specific power at all evaporation pressures. For the alkanes, a cycle with 30 mol% *n*-butane WF mixture performs best at most conditions. At very high evaporating pressures (> 34 bar), a cycle with 90 mol% *n*-butane WF mixture becomes optimal.

3.2.2 Absolute power output

From the previous results, ORC power systems are seen to have lower thermal efficiencies than those typically associated with large-scale, centralized fossil-fuelled power plants, due to the low temperature of the heat input involved. However, the ORC waste-heat energy source is more easily accessible, abundant and much more affordable than the fuel(s) used in conventional power plants. Fuel costs in such plants can, in some cases, account for up to 60 – 70% of the levelized costs of generating electricity over the lifetime of the plant's operation. Therefore, the aim in low-grade-heat-conversion technologies, at least from an economic viability perspective, becomes one of maximizing their power output while driving the dominant investment and capital costs of the systems down. Efficiency and other indices are important in as much as they contribute to this aim.

By optimizing the cycle (through maximizing the absolute power output) at different evaporation pressures, one arrives at the maximum power output achievable from the heat source using an ORC engine with the selected WFs. The ORC absolute power outputs with the WFs are presented in Fig. 5a (for *n*-butane + *n*-decane) and Fig. 5b (for *n*-perfluorobutane + *n*-perfluorodecane). The heat source used is seen to have the potential to deliver in excess of 20 MW of electricity when the alkanes (and their mixtures) are employed as the ORC WF; the perfluoroalkane cycles diver a maximum of about 16 MW. This presents a low-cost and viable energy source for most high-*T* process industries especially as no cost is incurred in fuel (*i.e.*, the heat source).

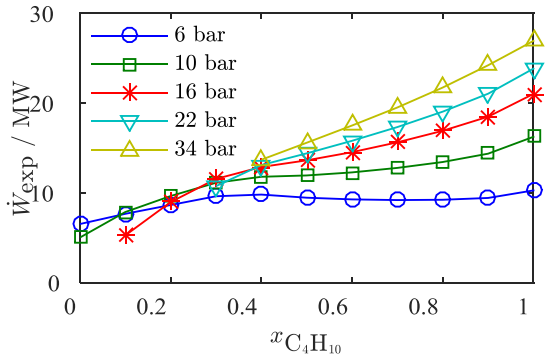


Fig. 5a: *Absolute power output of ORCs with alkane WFs*

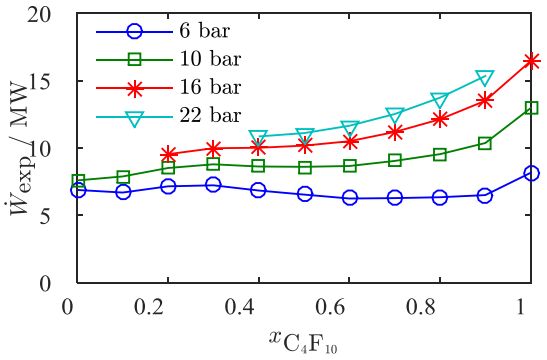


Fig. 5b: *Absolute power output of ORCs with perfluoroalkane WFs*

For both sets of WFs, the more-volatile component of the mixture generates the highest power output in the majority of the investigated cases as evidenced in Fig. 5. Amongst the alkanes, the ORC with pure *n*-butane delivers the highest power output while pure *n*-perfluorobutane delivers the highest amongst the perfluoroalkanes. The cycle with the less-volatile component of the binary mixtures (*n*-decane and *n*-perfluorodecane respectively) generally delivers the least power output. At evaporating pressures less than 6 bar (Fig. 5a), a WF mixture with 40 mol% *n*-butane performs best in comparison with other mixtures and the pure components. Similarly, for the perfluoroalkanes (Fig. 5b), a mixture with 30 mol% *n*-perfluorobutane performs best (at low evaporation pressures).

3.2.3 Optimal working fluid design

From the absolute power output (the primary selection index) results in Fig. 5, it would seem that the more-volatile pure components (*n*-butane or *n*-perfluorobutane) represent the optimal ORC WFs, especially for high-*P* and high power-output systems. However, cycles with WF mixtures are seen to deliver higher power outputs at low evaporation pressures; the mixtures also lead to cycles with higher power densities. Furthermore, using such WF mixtures at such low pressures limits the maximum allowable pressure of the ORC setup thus leading to a sizeable reduction in the ORC installation costs since high-*P* systems are generally known to be much more expensive than low-*P* systems. Also, in cases where low-*P* process requirements are dictated by other upstream/downstream processes in a facility, the WF mixtures provide an avenue to meet prescribed power demands as they deliver a higher power output than their single-component counterparts.

Therefore, the WF design (*i.e.*, the choice between a mixture and a single-component WF including the choice of the particular number of components and their compositions) is largely influenced by the cycle design – the heat source, the operating pressures and temperatures, the power output target and the intended application(s). This has been demonstrated with the ORC simulation results for the manageable case of two sets of single-component WFs and their mixtures as presented in Figs. 4 and 5. The cycle design may also be constrained by the choice of WF – for instance, its operating pressures or temperatures may be restricted due to flammability and degradability of the WF. Considering the numerous individual hydrocarbons and refrigerants from which such fluid mixtures can be designed, the eventual number of combinations grows exponentially with each additional fluid component, leading to a largely intractable problem. This presents a highly interwoven design problem that is best solved simultaneously with a structured approach.

Group-contribution EoS present a realistic opportunity to addressing this challenge [12, 14, 15]. In such EoS, properties of compounds are determined by the additive contributions from the individual molecular groups contained in the compound – individual group contributions are modelled separately. ORC WFs generally contain molecular groups that occur frequently in hydrocarbons and refrigerants (e.g. $-CH_3$, $-CH_2$, CF_2, $=CH$, $-CCl_2$). These groups form a much smaller set than the set of individual fluids they constitute – for example, the entire fluid family of normal alkanes (excluding methane) is composed of only two groups, *i.e.*, $-CH_3$, and $-CH_2$ groups. Thus with an efficient group-contribution approach, one can effectively design the combination of such molecular groups to

generate WFs while at the same time optimizing the ORC system design. For this work, we will employ the latest version of the SAFT group-contribution theories – the SAFT-γ Mie EoS.

4 Next Steps: CAMD with SAFT-γ Mie Group-Contribution Equation of State

In a similar manner to the SAFT-VR Mie, the SAFT-γ Mie EoS describes the interaction between two molecular groups using a Mie potential (Equation 1), where the group parameters retain their previous definitions (Section 2). Additional parameters for the molecular group description are the number of identical segments comprising a group, v^*, and the shape factor, S. The shape factor is a key parameter of the SAFT-γ Mie methodology that characterizes the extent to which the segments of a given group contribute to the overall molecular properties [17]. Intermolecular parameters for pure fluids (based on the *hetero-nuclear* molecular model) are derived from the contributions of the different groups that make up the molecule using combining rules. The required thermodynamic properties of such fluids are then derived via the Helmholtz free energy using standard thermodynamic relations.

SAFT-γ Mie parameters (including the 'like' and 'unlike' interaction parameters) for various molecular groups are available in published literature [18], including the -CH_3, -CH and the -CH_2 groups that are important for the description of hydrocarbon WFs chosen in the present ORC study. These parameters were derived by regression to experimental pure-component vapour-liquid equilibrium data. In Fig. 6 we present thermodynamic properties of pure alkanes and bubble-point curves of the *n*-butane + *n*-decane system generated using SAFT-γ Mie; these are compared with experimental data from the NIST database. It is clear that the SAFT-γ Mie group contribution EoS gives an accurate property description of both pure fluids and the mixture thereby giving confidence that the SAFT methodology can be extended to other candidate WFs for which the molecular/group parameters are yet to be derived. This is especially remarkable as the properties (enthalpies and entropies) plotted in Fig. 6 were not used in the estimation of the group model parameters.

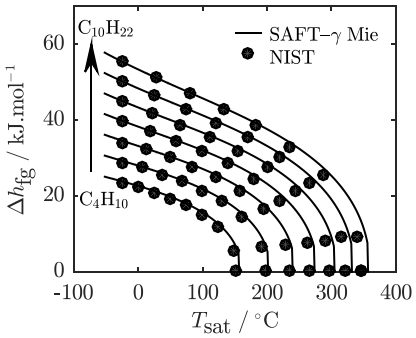


Fig. 6a: *Phase change enthalpies of normal alkanes*

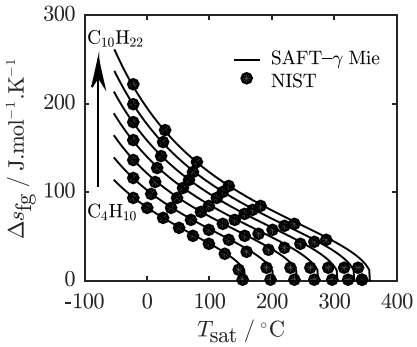


Fig. 6b: *Phase change entropies of normal alkanes*

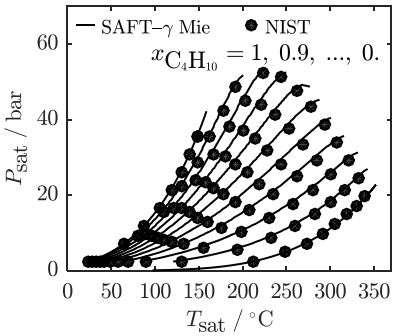


Fig. 6c: *P-T bubble-point curves of n-butane + n-decane systems*

Important groups yet to be modelled include those associated with refrigerants, other halogenated hydrocarbons and siloxanes (e.g., -CF_3, -CF_2 and -CCl groups). Once these are accounted for within the SAFT-γ Mie group contribution framework, they will be included in the database of candidate groups for WF design, thus enabling a larger and more rigorous design set for the CAMD approach.

A general CAMD structure for ORC design is illustrated with the flowchart in Fig. 7. A key feature of this structural approach is the incorporation of the WF design and the ORC design in a single mixed-integer non-linear optimization problem (MINLP) for which solution algorithms are readily available. Such a formulation would thereby result in simultaneous optimal WF and optimal cycle configuration satisfying all process (heat source/sink, pinch conditions, downstream requirements) and environmental (GWP, ODP, toxicity, *etc*.) constraints. Additionally, molecular groups that favour higher cycle performance would be identified for further investigation. Furthermore, sensitivity analyses can be provided for such optimal WF and cycle designs with the view to capturing changes in optimal solutions/configurations with unforeseen fluctuations in process conditions (*e.g.*, heat source/sink temperature and flowrate variations).

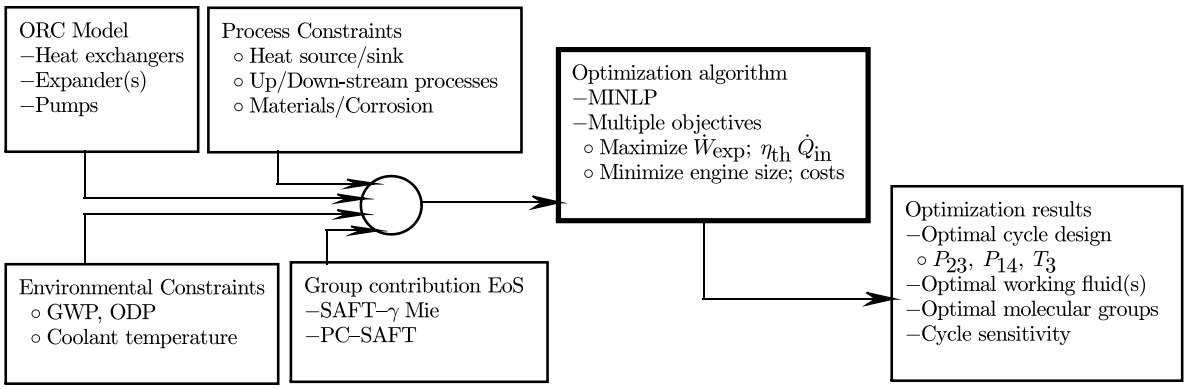


Fig. 7: *A computer-aided molecular-design (CAMD) structure for ORC power-systems*

5 Conclusions

The present study is aimed at developing a framework for the computer-aided molecular design (CAMD) of working fluids (WFs) for organic Rankine cycle (ORC) power-generation systems in low-grade-heat-conversion applications. An essential component of such designs is an analytical equation of state (EoS). Thus, in the first instance, we assess the suitability of the SAFT-VR Mie equation of state for the provision of the thermodynamic properties of ORC WFs – both single-component and multi-component fluids, and later on we consider the SAFT-γ Mie group contribution EoS, which accurately predicts the thermodynamic properties of WFs (and mixtures) via contributions from the individual molecular groups. Mixture WFs provide the opportunity of an improved thermal match to the heat source and sink by exhibiting non-isothermal phase-change behaviour. This way, the average temperature difference (and associated exergy loss) during heat addition and rejection is minimized, which can lead to an enhancement of the ORC power output and efficiency.

The molecular basis of the SAFT equations and their firm foundation in statistical mechanics indicate that the approach could be an attractive alternative to those commonly used in the analysis of ORCs, such as REFPROP or CoolProp, for fluids that are not included in those databases, or for which significant uncertainties may be indicated. By using two sets of mixtures – one of alkanes, comprising *n*-butane and *n*-decane, and one of perfluoroalkanes, comprising *n*-perfluorobutane and *n*-perfluorodecane – the SAFT-VR Mie EoS is shown to accurately describe the relevant thermodynamic properties of ORC WFs, especially in *T-s* or *P-h* spaces. Moreover, the SAFT-γ Mie EoS also presents excellent results for pure alkanes and their mixtures, despite the fact that only a limited number of parameters were used to define the molecular groups. Based on these observations, it can be concluded that the SAFT modelling approach is an appropriate tool for the provision of thermodynamic WF information in the analysis of engineering cycles, such as ORCs.

For the case of a refinery flue gas waste-heat source, ORC calculations based on thermodynamic information generated from the SAFT-VR Mie EoS indicate a potential (electrical) power in excess of 20 MW, based on the recovery of 200 MW_{th}. However, the choice of the optimal WF is not trivial, with various indices and operating conditions/constraints resulting in different optimal fluids varying between the single-component (pure) fluids and the working-fluid mixtures. The more-volatile pure fluids (*n*-butane and *n*-perfluorobutane) appear to lead to ORC systems with the highest thermal efficiencies and lowest expansion ratios, while a variety of WF mixtures lead to ORCs with the highest power densities (power output per unit mass flowrate). Ultimately, in the opinion of the present authors, the absolute power output remains the key thermodynamic index for waste heat recovery systems, and once again, the more volatile pure fluids were the preferable ORC WFs in this regard; only at low evaporation pressures do the mixtures perform better.

References

[1] C. N. Markides, The role of pumped and waste heat technologies in a high-efficiency sustainable energy future for the UK, Appl. Therm. Eng. 53 (2013) 197-209.
[2] LLNL. Estimated energy use in 2013. https://flowcharts.llnl.gov/index.html. Accessed 28/12/15.

[3] Estimated energy use in the European Union in 2006. http://www.sankey-diagrams.com/european-energy-flows-sankey. Accessed 28/12/15.
[4] I. I. Novikov, The efficiency of atomic power stations, J. Nucl. Energy 7 (1958) 125-128.
[5] F. L. Curzon, B. Ahlborn, Efficiency of a Carnot engine at maximum power output, Am. J. Phys. 43 (1975) 22-24.
[6] N.A. Lai, M. Wendland, J. Fischer, Working fluids for high-temperature organic Rankine cycles, Energy 36 (2011) 199-211.
[7] S. Sami, Energy and exergy analysis of new refrigerant mixtures in an organic Rankine cycle for low temperature power generation, Int. J. Ambient Energy 31 (2010) 23-32.
[8] H. Chen, D.Y. Goswami, E.K Stefanakos, A review of thermodynamic cycles and working fluids for the conversion of low-grade heat, Renewable Sustainable Energy Rev. 14 (2010) 3059-3067.
[9] G. Angelino, C. Invernizzi, Cyclic methylsiloxanes as working fluids for space power cycles, J. Sol. Energy Eng. 115 (1993) 130.
[10] U. Drescher, D. Brüggemann, Fluid selection for the organic Rankine cycle (ORC) in biomass power and heat plants, Appl. Therm. Eng. 27 (2007) 223-228.
[11] B. Liu, K. Chien, C. Wang, Effect of working fluids on organic Rankine cycle for waste heat recovery, Energy 29 (2004) 1207-1217.
[12] M. Lampe, J. Gross, A. Bardow, Simultaneous process and working fluid optimisation for organic Rankine cycles using PC-SAFT, Eur. Symp. Comput. Aided Process Eng. 30 (2012) 572-576.
[13] O. A. Oyewunmi, A. I. Taleb, A. J. Haslam, C. N. Markides, An assessment of working-fluid mixtures using SAFT-VR Mie for use in organic Rankine cycle systems for waste-heat recovery, Comput. Therm. Sci. 6 (2014) 301-316.
[14] A. I. Papadopoulos, M. Stijepovic, P. Linke, On the systematic design and selection of optimal working fluids for organic Rankine cycles, Appl. Therm. Eng. 30 (2010) 760.
[15] A. I. Papadopoulos, M. Stijepovic, P. Linke, P. Seferlis, S. Voutetakis, Multi-level design and selection of optimum working fluids and ORC systems for power and heat cogeneration from low enthalpy renewable sources, Comput. Aided Chem. Eng. 30 (2012) 66.
[16] T. Lafitte, A. Apostolakou, C. Avendao, A. Galindo, C. S. Adjiman, E. A. Muller, G. Jackson, Accurate statistical associating fluid theory for chain molecules formed from Mie segments, J. Chem. Phys. 139 (2013) 154504.
[17] V. Papaioannou, T. Lafitte, C. Avendaño, C. S. Adjiman, G. Jackson, E. A. Muller, A. Galindo, Group contribution methodology based on the statistical associating fluid theory for heteronuclear molecules formed from Mie segments, J. Chem. Phys. 140 (2014) 054107.
[18] S. Dufal, V. Papaioannou, M. Sadeqzadeh, T. Pogiatzis, A. Chremos, C. S. Adjiman, A. Galindo, Prediction of thermodynamic properties and phase behavior of fluids and mixtures with the SAFT-γ Mie group-contribution equation of state, J. Chem. Eng. Data 59 (2014) 3272-3288.
[19] G. Soave, Equilibrium constants from a modified Redlich-Kwong equation of state, Chem. Eng. Sci. 27 (1972) 1197-1203.
[20] D. Y. Peng, D. B. Robinson, A new two-constant equation of state, Ind. Eng. Chem. Fundam. 15 (1976) 59-64.
[21] W. G. Chapman, K. E. Gubbins, G. Jackson, M. Radosz, SAFT: equation-of-state solution model for associating fluids, Fluid Phase Equilib. 52 (1989) 31-38.
[22] O. A. Oyewunmi, A. Taleb, A. J. Haslam, C. N. Markides, On the use of SAFT-VR Mie for assessing fluorocarbon working-fluid mixtures in organic Rankine cycles for waste-heat recovery, 2nd International Seminar on ORC Power Systems (2013).
[23] E. W. Lemmon, M. L. Huber, M. O. McLinden, NIST reference fluid thermodynamic and transport properties database, http://www.nist.gov/srd/upload/REFPROP9.PDF Accessed 28/12/15.
[24] H. H. Reamer, B. H. Sage, Phase equilibria in hydrocarbon systems. Phase behavior in the n-butane - n-decane system, J. Chem. Eng. Data 9 (1964) 24-28.
[25] J. M. H. Levelt-Sengers, Critical exponents at the turn of the century, Physica 82 (1976) 319-351.